

DSC/TG OF Al-BASED ALLOYED POWDERS FOR P/M APPLICATIONS

DSC/TG PRAHOV NA OSNOVI Al PRIMERNIH ZA P/M UPORABO

Borivoj Šuštaršič¹, Jože Medved², Srečko Glodež³, Marko Šori³, Albert Korošec⁴

¹Institute of Metals and Technology, Lepi pot 11, 1000 Ljubljana, Slovenia

²OMM, NTF, University of Ljubljana, Aškerčeva 12, 1000 Ljubljana, Slovenia

³University of Maribor, FNM, Koroška cesta 160, 2000 Maribor, Slovenia

⁴Talum, Tovarna aluminija d. d., Tovarniška cesta 10, 2325 Kidričevo, Slovenia

borivoj.sustarsic@imt.si

Prejem rokopisa – received: 2013-11-13; sprejem za objavo – accepted for publication: 2014-04-16

Al-based alloyed powders, appropriate for the sintering procedure (powder metallurgy, P/M) contain the alloying elements with a high solid solubility in Al, enabling reaction and liquid-phase sintering. They are surface oxidised because of a high affinity of Al to oxygen. Besides, this type of powders contains a polymeric lubricant (wax), which reduces the friction on die walls during automatic die compaction into the final compact shape of a product. This lubricant has to be removed slowly during the first stage of sintering in order to prevent deformations and cracking of the product. Consequently, its sintering is very complex. Generally, these powders are sintered in pure nitrogen with a low dew point. The optimum sintering conditions are generally determined on the basis of light and scanning electron microscopy. The investigation can also be completed very successively with differential scanning calorimetry and thermo gravimetry. The first one allows an insight into the endo- and exothermic reactions, taking place during the heating and cooling of a compacted metal powder, and the second one allows an insight into the processes, connected with the mass loss (a reduction, a lubricant removal, etc.) or mass increase (an oxidation). The DSC/TG of three commercial Al-based alloyed powders was performed in the frame of our investigations. The results were compared with the theoretical thermodynamic-based calculations and the optimum sintering conditions were proposed.

Keywords: Al-based alloyed powders, sintering, differential scanning calorimetry and thermo gravimetry (DSC/TG)

Legirani prahovi na osnovi Al, primerni za sinter postopek (P/M, metalurgija prahov), vsebujejo zlitinske elemente z veliko topnostjo v trdnem Al, kar omogoča reakcijsko sintranje v prisotnosti tekoče faze. Zaradi velike afinitete aluminija do kisika so na površini oksidirani. Poleg tega vsebujejo ti prahovi polimerno mazivo, ki zmanjšuje trenje na stenah orodja med avtomatskim stiskanjem prahu v končno oblikovan izdelek. To mazivo moramo v prvi fazi procesa sintranja počasi odstraniti, sicer bi lahko prišlo do nepopravljive deformacije ali celo pokanja izdelka. Zato je njihovo sintranje zelo zahtevno. Navadno se sintrajo v čisti dušikovi atmosferi z nizko temperaturo rosišča. Poleg fizikalno-kemijske karakterizacije sintranih izdelkov s svetlobno in elektronsko mikroskopijo je za določitev optimalnih pogojev sintranja zelo uporabna diferencialna vrstična kalorimetrija, kombinirana s termogravimetrijo (DSC/TG). Prva omogoča vpogled v endo- in eksotermne reakcije, ki potekajo med segrevanjem in ohlajanjem kompaktnega kovinskega prahu, druga pa s temi procesi povezano izgubo (redukcija, odstranitev maziva itd.) ali prirastek (oksidacija) mase. V okviru naših raziskav smo izvedli DSC/TG treh komercialno dosegljivih prahov na osnovi Al, ugotovljene reakcije smo primerjali z napovedmi teoretične termodinamike in predlagali optimalne pogoje sintranja teh prahov.

Ključne besede: prahovi zlitine na osnovi Al, sintranje, diferencialna vrstična kalorimetrija s termogravimetrijo

1 INTRODUCTION

Al-based alloyed powders, appropriate for the sintering procedure (powder metallurgy, P/M) contain the alloying elements (Cu, Zn, Mg, etc.) with a high solid solubility in Al enabling reaction and liquid-phase sintering. Generally, these powders are surface oxidised because of a high affinity of Al to oxygen. Besides, these types of powders contain mass fraction approximately $w = 1.5\%$ of a polymeric lubricant, which reduces the friction on die walls during automatic die compaction (ADC) into the final compact shape of a product. This lubricant has to be removed slowly during the first stage of sintering in order to prevent deformations and cracking of the product. Therefore, its sintering is very complex. Generally, these types of powders are sintered in pure nitrogen (N_2 , 5.9) with a low dew point (below $-40\text{ }^\circ\text{C}$). The optimum sintering conditions are commonly determined on the basis of light (LM) and scanning electron microscopy combined with a microchemical

analysis based on the measurement of the dispersed kinetic energy of X-rays (an energy dispersive X-ray spectrometer – SEM/EDS).¹ The investigation can also be completed very successively with heating microscopy, as well as differential scanning calorimetry and thermo gravimetry (DSC/TG). The DSC method allows an insight into exothermic/endothemic reactions, and the TG method allows an insight into the mass increase/decrease occurring during the heating/cooling of a compact, respectively.

DSC is an effective and widely used method of the thermal analysis (TA) of metallic and other materials. It is a modern, completely automated and highly improved version of an older method known as differential thermal analysis (DTA) where the temperature differences between the investigated and the standard (neutral, usually alumina) samples are measured. The temperature differences are the consequence of the heat release/consume of the exothermic/endothemic reactions associated with different physical and chemical processes (melting, soli-

dification, evaporation, oxidation, reduction, solid-state transformations, etc.) occurring during the heating and cooling of the investigated sample. The actual difference between the DTA and DSC methods is a more precise determination of the released or consumed heat. With the DSC method it is possible to determine the released or consumed heat much better because the specific heats and their temperature dependencies of the investigated samples are considered. The new DSC devices also have a significantly higher number of temperature sensors (thermocouples) in a very small space of the measuring cell and an improved calibration system of the thermal buoyancy, enabling a much better measuring of temperature gradient dT/dt ($^{\circ}\text{C/s}$). The measuring cell is usually placed on a very precise balance. This also enables thermogravimetry (TG) and a simultaneous tracking of the mass changes due to different reactions. Modern DSC/TG devices enable experimental work with a controlled heating/cooling rate in different stationary or flow atmospheres. They enable the heating up to very high temperatures (for the metals, generally, up to 1600°C ; the maximum of 2400°C is also possible). Mass changes are the results of the changes in the investigated sample (a wax removal, an evaporation, etc.) or its reaction with the selected atmosphere (hydrogen, oxygen, water vapour, etc.).

The DSC/TG analyses of three commercial² Al-based alloyed powders were performed in the frame of our investigations. The results were compared with the theoretical thermodynamic-based calculations (ThermoCalc)³ and the optimum sintering conditions were proposed. Our experiments were performed with a Netzsch STA (simultaneous thermal analysis) device, Germany.^{4,5}

2 EXPERIMENTAL WORK

The actual chemical compositions of the selected commercial Al powders are given in **Table 1**. From this table one can notice that the first AlCuSiMg-based alloy (A) is of type 2xxx (2014), the second alloy (B) is a special hypereutectoid Al-Si-based alloy with a high Si content and additions of Cu and Mg. The third alloy (C) is an AlZnMgCu-based alloy of 7xxx family type (7075). The powders were compacted on an ADC mechanical press (Dorst, Germany, 60 kN) with a 450 MPa pressure into standard tensile-test specimens (DIN ISO 2740).⁶ Thirty-five (35) pieces of each alloy were prepared for

further experiments and investigations. From three (3) characteristic specimens (with the average green density) samples of approximately 5 g were cut off for the DSC/TG experiments. As already mentioned, the experiments were performed with a Netzsch STA 449C Jupiter⁵ device installed at the Laboratory for Thermodynamics of Materials, Department for Metallurgy and Materials, University of Ljubljana. This equipment enables a simultaneous performance of differential scanning calorimetry and thermogravimetry with the selected heating/cooling rate and atmosphere conditions. In our case the samples were heated/cooled at the constant rate of 5°C/min in a stationary atmosphere of Ar (the purity of 5.9), as well as in a flow atmosphere (10 mL/h) of pure nitrogen (5.9). The samples were heated up to the maximum temperature of 650°C and then cooled down. The calibration (determination of the base line) of the device as well as the evacuation of the cell were performed every time before the start of an analysis.

Table 1: Actual average chemical compositions of the selected powders in mass fractions (w/%)

Tabela 1: Povprečna kemijska sestava izbranih prahov v masnih deležih (w/%)

Designation	Cu	Si	Mg	Zn	Al	Remarks
Chemical composition	w/%					
Alloy A	4.5	0.62	0.48	–	bal	0.08 % Fe
Alloy B	2.7	15.0	0.58	–	bal	
Alloy C	1.6	–	2.40	5.8	bal	0.29 % Sn

The average bulk chemical compositions of the powders were determined with a classical Agilent 720 ICP-OES (ion coupled plasma - optical emission spectroscopy) instrument with a limit of detection ($< 0.001\%$ of an individual element). However, the microchemical compositions of individual powder particles were determined with SEM/EDS (a JEOL FE HR JSM-6500F and Oxford EDS INCA Energy 450, X-Sight LN2 detector).

The compacted tensile-test specimens were also sintered at the selected sintering conditions. The obtained mechanical properties are given in **Table 2**. They are in accordance with the expectations and the powder-producer specifications.²

The standard metallographic samples of the powders and sintered materials were prepared for the microstructural and microchemical investigations under LM and SEM/EDS. In this article, the description is focused

Table 2: Average mechanical properties of the materials after the ADC and sintering of the tensile-test specimens made of the selected Al-based powders

Tabela 2: Povprečne mehanske lastnosti materialov, dobljene po stiskanju in sintranju nateznih preizkušancev iz izbranih Al-prahov

Alloy	Green density	Sintered density	Hardness HB _{2,5/31,25}	Tensile strength	Yield strength	Young's modulus	Elongation %
	g/cm ³			MPa			
A	2.62	2.60	65	202	156	3834	2.23
B	2.52	2.62	104	239	219	4399	0.70
C	2.61	2.73	102	325	250	4102	3.90

mainly on DSC/TG investigations and analyses. The description of the other investigations can be found elsewhere.¹

3 RESULTS AND DISCUSSION

This article will only focus on some general characteristics and the most important findings. An additional description of the results of the investigations can be found elsewhere.¹ **Figure 1** shows the typical measuring protocol and the results of the DSC analysis obtained for both experimental conditions during the investigation of alloy A. The heating/cooling program is recorded with a fine dotted line. One can notice that the resulting DSC curve for the analysis performed with stationary Ar is almost the same as the one performed with a flow of nitrogen. Only small differences can be noticed. They can be ascribed to the fluctuations in the sample composition, solubility of gas in the melt, possible formation of nitrides/oxides and variations of the used experimental conditions. The sole large exothermic (exo) and equivalent endothermic (endo) peaks can be ascribed to the melting and solidification of the alloy, respectively. The exo peak connected with the solidification is sharper for the nitrogen-flow experiment. Other changes are less distinctive and can be observed only in the magnified mode. The cooling parts of the DSC curves have no visible additional peaks, which means that, during the melting, the homogeneous alloy was completely formed, without any significant precipitation of the secondary phases during the cooling of the sample.

Figure 2 shows the heating part of the DSC curve in the magnified mode obtained with the DSC analysis of alloy A. In the temperature region between 100 °C and 500 °C there is a number of small less recognizable endo peaks. The first one at 138 °C (i.e., 141 °C; the data for the experiments in stationary Ar is given in parentheses) can be associated with the beginning of the melting of the polymer wax, but the later peaks at ((261), 322 (328), (348) and 440 (442)) °C are the results of the evapora-

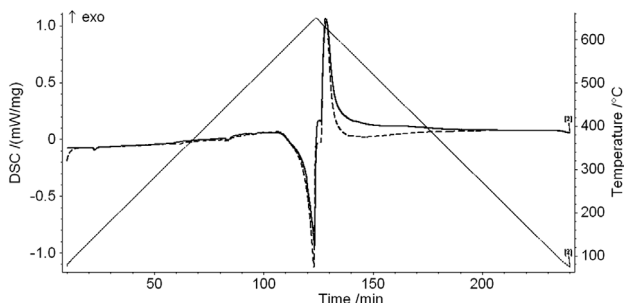


Figure 1: Measuring protocol of the DSC analysis of alloy A (heating/cooling is shown with a fine dotted line), a comparison of the DSC curves obtained during the experiments performed in stationary Ar (dashed line) and in a flow of N₂ (full line)

Slika 1: Merilni protokol DSC-analize zlitine A (segrevanje/ohlajanje – fina pikčasta črta); primerjava DSC-krivulj, izdelanih v stacionarnem argonu (črtkana črta) in pretoku dušika (polna črta)

tion of the multicomponent lubricant system. A constant slight ascent of the DSC curve in this temperature region can also be noticed. This is the result of the exothermic nature of the wax removal (burning). Simultaneously, at the temperatures above 400 °C, above the solvus line of the complex alloying system, one can also expect the beginning of the formation of the final solid solution (α -Al) because of the increased diffusion of the alloying elements into the aluminium. The SEM/EDS microchemical analyses of loose powders showed¹ that not all the individual (pre-alloyed) powder particles are of the same chemical compositions, but they are of different compositions forming the final mixtures with the average compositions given in **Table 1**. For example, SEM/EDS analyses¹ showed that alloy A consisted of the powder particles of pure Al, alloys Al-10Si-Mg (but Mg was not detected) and Cu-5Al. Alloy B consisted of the powder particles made of the Al-3Si, Al-27Si-1Mg-6Cu and Si-Al-based alloys, and, finally, alloy C consisted of the particles of pure Al and the particles of the Al-Zn-Mg-Cu alloy (approximately $w(\text{Al}) = 79\%$, $w(\text{Mg}) = 5\%$, $w(\text{Cu}) = 4\%$, $w(\text{Zn}) = 12\%$). Thus, the endo peaks at approximately (452, 486, 482 (484) °C and 506 (509)) °C can be associated with the diffusion of the alloying elements and the formation of the α -Al solid solution. EDS analyses also showed that alloy B had the most oxidised particles (a high Si content) and alloy C was the least oxidised of all.

The theoretical calculation of the thermodynamic equilibrium with ThermoCalc³ predicts the formation of the first melt at 525 °C (**Figure 3**). On the experimental DSC curve, it is visible at 534 °C. However, the real large endo peak caused by the melting starts at 567.8 (573.2) °C and finishes at approximately 640 °C when the melting of the alloy is completed. ThermoCalc predicts the two-phase region (α -Al+L) between 525 °C and 638 °C (**Figure 3**). This is in a relatively good agreement with the experimental results of the DSC analysis. From these results one can find that the optimum liquid-phase sintering temperature is somewhere in the middle of the α -Al+L region. This is in a good agreement with the powder producer that recommends, for

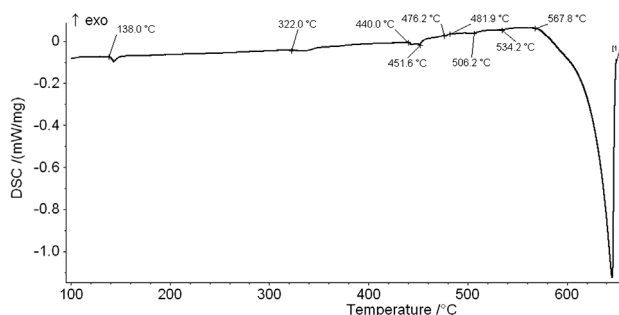


Figure 2: Heating part of the DSC curve of alloy A, protective atmosphere of N₂ 5.9, flow of 10 mL/h, 1 × vacuum, $T_{\text{max}} = 650$ °C, 5 °C/min
Slika 2: DSC segrevalna krivulja zlitine A, zašč. atm. N₂ 5,9, pretok 10 mL/h, 1 × vakuum, $T_{\text{maks.}} = 650$ °C, 5 °C/min

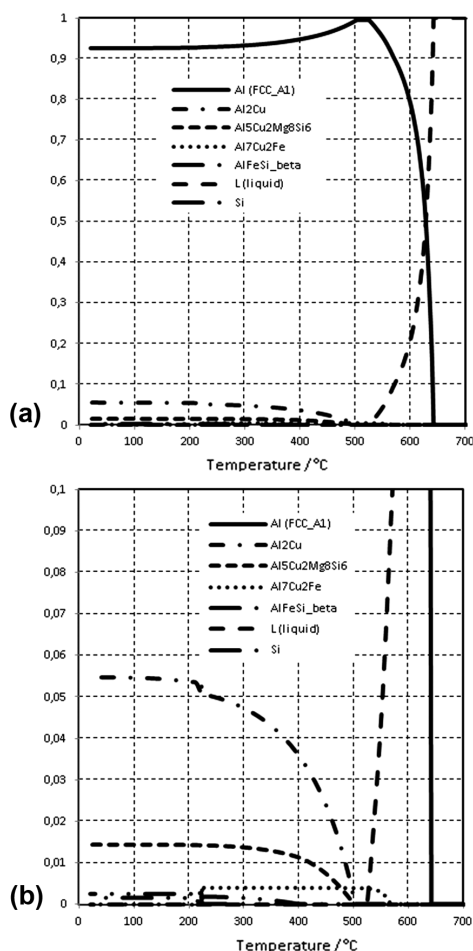


Figure 3: a) Theoretical equilibrium thermodynamic phase stability of alloy A and b) detail of the diagram up to a fraction of 0.1 mol, calculated with ThermoCalc³

Slika 3: a) Teoretična ravnotežna termodinamska stabilnost faz zlitine A in b) detajl v diagramu do 0,1 molskega deleža, izračunano z orodjem ThermoCalc³

alloy A, a sintering temperature between 590 °C and 600 °C. In this case most of the intermetallic phase is already dissolved in the solid solution of Al and a small amount of the liquid needed is also present.

The thermodynamic analysis with ThermoCalc also shows (Figure 3) that, in the equilibrium, alloy A contains solid crystals of the homogeneous solid solution of α -Al from room temperature up to 638 °C and mainly intermetallic phase Al₂Cu (the θ phase) up to 501 °C. As already mentioned, the first liquid appears at 525 °C.

The theory also predicts possible formations of phases Al₅Cu₂Mg₈Si₆ (up to 500 °C), Al₇Cu₂M (M = Fe, up to 565 °C), β AlFeSi (up to 223 °C) and Si up to 396 °C. From this analysis one can conclude that alloy A is a typical precipitation-hardening alloy. Therefore, an improvement in the mechanical properties of this alloy can be achieved with a combination of homogenization annealing at the temperature of a complete solid solution (for example, 500 °C, 20 min), fast cooling and natural (T4) or artificial ageing (T6, for example, 150 °C, 15 min). The optimization of the ageing parameters can be performed with the help of theoretical and experimental CCT (continuous-cooling temperature) diagrams. The optimum process parameters (temperature/time) of ageing lead to an alloy with a fine uniform dispersion of the precipitates of the intermetallic phases in the α -Al solid solution. In the case of high cooling rates (10³ °C/h) only a formation of very fine GP (Guiner-Preston) zones and, eventually, a fine θ' (Theta prime) phase can be expected. Lower cooling rates are undesirable because of the formation of other larger intermetallic phases such as S' or θ phases.^{7,8}

The experimental cooling DSC curve (Figure 4) shows only one large exo peak with its beginning at 637.9 (637.2) °C, which is the result of the sample solidification during cooling. The solidification is finished between approximately 580 °C and 590 °C. Later, only one, almost invisible exo peak appears at approximately 570.1 (563.5) °C. This could be associated with the precipitation of intermetallic phases. The precipitation of phases Al₂Cu and Mg₂Si is possible during a relatively slow cooling (5 °C/min). This could only be confirmed

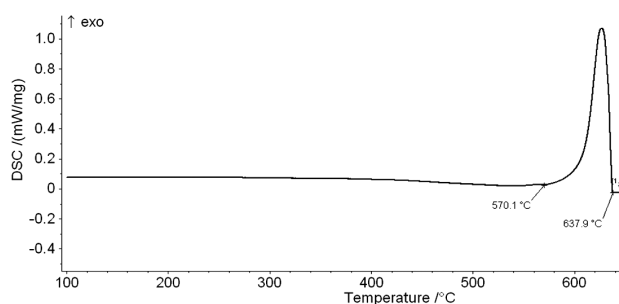


Figure 4: Cooling DSC curve of alloy A, protective atmosphere of N₂ 5,9, flow of 10 mL/h, 1 × vacuum, T_{max} = 650 °C, 5 °C/min

Slika 4: Ohlajevalna DSC-krivulja zlitine A, zaščitna atmosfera N₂ 5,9, pretok 10 mL/h, 1 × vakuum, T_{maks} = 650 °C, 5 °C/min

Table 3: Comparison of the results of DSC analyses in the flow of N₂ for the selected powders

Tabela 3: Primerjava rezultatov izvedenih DSC-analiz v toku N₂ za izbrane prahove

Alloy	Dewaxing*			Alloy formation*			Melting*		Solidification**	
	(temperature, °C)			(temperature, °C)			(temperature, °C)		(temperature, °C)	
	Start	Intermediate	Finish	Start	Intermediate	Finish	Start	Finish	Start	Finish
A	138	348	447	440	506.2	534.2	567.8	650	637.9	570.1
B	138	344	426	498	509.0	-	526.0	600	520.0	615.0
C	139	332	406	466	-	-	542.0	655	542.0	638.0

* endo peaks, ** exo peaks

Table 4: Theoretical temperature thermodynamic phase stability of the selected alloying systems, calculated with ThermoCalc³**Tabela 4:** Teoretična temperaturna termodinamska stabilnost faz v izbranih zlitinskih sistemih, izračunana z orodjem ThermoCalc³

Designation temperature, °C	α -Al	Al ₂ Cu	Al ₅ Cu ₂ Mg ₈ Si ₆	Al ₇ Cu ₂ M	Si	AlFeSi_Beta	Mg ₂ X_Cl	S_Al ₂ CuMg	MgZn ₂	T_AlCuMgZn	α -Al + L	L
Alloy A	< 637.8	< 501.0	< 500	223.2–565.0	< 395.8	< 223	–	–	–	–	525.0–637.8	> 525.0
Alloy B	< 562.6	< 447.8	< 526	–	< 619.7	–	–	–	–	–	532.6–562.6	> 532.6
Alloy C	< 630.0	–	–	–	–	–	< 511.1	< 442.7	< 409.7	> 250.1	516.5–630.0	> 516.5

with XRDS (X-ray diffraction spectroscopy) of the metallographic samples (not performed yet).

The results of the DSC experiments for alloys B and C are compared with the ones for alloy A in **Table 3**. The theoretical calculations of the thermodynamic equilibrium performed with ThermoCalc were also obtained for alloys B and C. The temperatures of the thermodynamic stability of all the phases are given in **Table 4**.

Figure 5 shows a typical measuring protocol and the results of the TG analysis obtained for both experimental conditions during the investigation of alloy A. The heating/cooling program is recorded with a dashed line. One can notice that the resulting TG curve for the analysis performed with stationary Ar is almost the same as the one performed with the flow of nitrogen. The cooling part of the TG curve shows no changes and can, therefore, be omitted. **Figure 6**, therefore, shows only the heating TG curve of alloy A obtained for the flow of nitrogen.

From **Figure 6** one can clearly see that the mass decrease starts at 248 (247) °C because of the lubricant removal (dewaxing). It is completely finished at 447 (446) °C. The total mass loss in this temperature region is 1.42 (1.38) %. This result is in accordance with the powder-producer specification (the wax content $w = 1.5$ %) considering the fluctuation of the wax content inside the volume of the compacted tensile-test specimen. Surprisingly, the mass of the sample again starts to increase

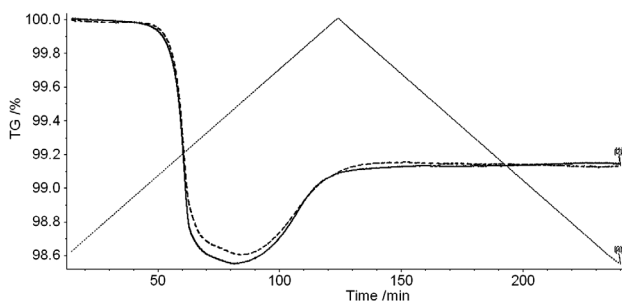


Figure 5: Measuring protocol of the TG analysis of alloy A (heating/cooling is presented as a fine dotted line), comparison of the TG curves obtained during the experiment performed in stationary Ar (dashed line) and the flow of N₂ (full line)

Slika 5: Merilni protokol TG-analize zlitine A (segrevanje/ohlajanje – pikčasta črta), primerjava TG-krivulj, dobljenih med preizkusom v stacionarnem pretoku Ar (črtkana črta) in pretoku N₂ (polna črta)

after dewaxing up to $w = 0.53$ (0.48) %. At the higher temperatures, a reoxidation of the sample is possible and most likely to happen. The first experiments were performed in the pure stationary Ar, and the first assumption was that either the entrapped vapour of the wax caused the sample to reoxidise, or a small leakage of the cell occurred. Therefore, the new DSC/TG experiments were performed in the flow of nitrogen. As one can see, the results of the analyses are very similar (**Figure 6**) and the final conclusion is that the reoxidation is a consequence of the entrapped molecules of air in the green compact because the released vapours of the wax are removed from the cell together with the flow of nitrogen.

The powder producer recommends the following dewaxing procedure during the sintering process: the flow of N₂ in the temperature region between 380 °C and 420 °C for 20 min. However, our TG experiments show that the dewaxing starts much earlier (at approximately 245 °C) and finishes later (at approximately 450 °C). The process of dewaxing must be, therefore, optimized by adequately slowing down the heating procedure in this temperature region. The results of the TG experiments involving alloys B and C are compared with the ones for alloy A in **Table 5**. Dewaxing of the samples made of the green compacts of alloys B and C starts at even lower temperatures (below 200 °C) in the case of the TG performed with stationary Ar. In spite of this, dewaxing of the green compacts made of these materials can be performed in the same way as for alloy A. An interesting result of the TG analyses is that alloy (pow-

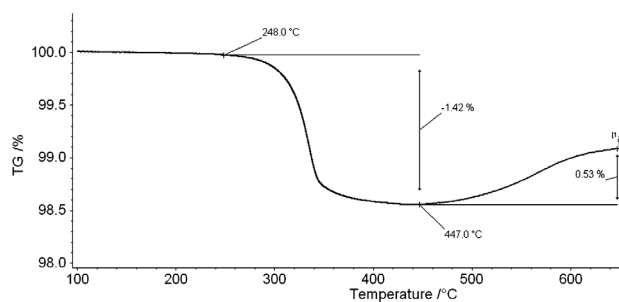


Figure 6: Heating TG curve of alloy A, protective atmosphere of N₂ 5.9, flow of 10 mL/h, 1 × vacuum, $T_{\max} = 650$ °C, 5 °C/min

Slika 6: Segrevalna TG-krivulja zlitine A (sprememba mase vzorca med segrevanjem), zašč. atm. N₂ 5,9, pretok 10 mL/h, 1 × vakuum, $T_{\max} = 650$ °C, 5 °C/min

Table 5: Comparison of the results of the TG analyses of the selected powders**Tabela 5:** Primerjava rezultatov izvedenih TG-analiz izbranih prahov

Designation	Dewaxing			Reoxidation			Remarks
	Start	Finish	Mass decrease	Start	Finish**	Mass increase	
	°C		w/%	°C		w/%	
Alloy A	248 (247)*	447 (446)	1.40 (1.38)	447 (446)	650	0.53 (0.48)	–
Alloy B	249 (194)	426 (477)	1.53 (1.93)	426 (477)	650	0.25 (0.14)	Early start and late finish of dewaxing in Ar
Alloy C	249 (198)	426 (463)	1.38 (1.73)	426 (463)	650	1.38 (1.92)	

* ... Results of the experiments performed in stationary Ar are given in parenthesis

** ... All experiments finished at 650 °C

der) C with the lowest original oxidation was reoxidised the most during the TG test and that alloy B with the highest original oxidation was reoxidised the least during the TG test. One can speculate that, under the given conditions (time/temperature/atmosphere), each Al-based alloy has a specific oxidation potential if exposed to oxygen.

SEM/EDS analyses¹ showed that powder particles are surface oxidised and that the selected powders are mixtures of different alloys. During ADC some molecules of air are also entrapped. The exact wax composition is not known and it is, therefore, difficult to determine the nature of its melting, evaporation and oxidation. Generally, it is the producer's know-how. But, the waxes appropriate for ADC generally consist of multicomponent systems. The performed DSC/TG analyses can give only the basic but important information about the optimization of dewaxing and sintering processes, respectively.

4 CONCLUSIONS

In the frame of the present work the theoretical thermodynamic analyses and microstructure characterization of the selected Al-alloyed powders are completed with DSC/TG analyses. These provide a more precise insight into the events occurring during the heating and cooling of the green compacts made of the selected Al powders, as well as the optimization of the sintering process. The investigations show that DSC/TG experiments must be performed very carefully and must be, as much as possible, similar to the performed sintering procedure. In the first heating phase, the mass of the samples gradually decreases because of dewaxing. This is associated with the endo (melting and evaporation) and exo (burning) reactions detected on DSC heating curves. Unexpectedly, in all the cases the increase in the sample mass starts above approximately 450 °C. The most probable reason for this is the reoxidation of the samples with the molecules of air entrapped in the green compact. DSC analyses have also shown when exactly, during the heating,

the solution of the alloying elements is formed and the homogeneous solid solution of α -Al, the formation of the first melt, takes place, and when the general melting of the sample starts and finishes. During cooling, DSC analyses have shown the start and finish of the solidification, also indicating when the precipitation of the secondary intermetallic phases occurs at a given cooling rate. These analyses were completed with the theoretical thermodynamic calculations that allow a better understanding of the microstructure evolution, the optimization of heat treatment (precipitation hardening) and an improvement in the mechanical properties.

Acknowledgement

The authors wish to thank the Slovenian Research Agency for the financial support in the frame of project No. L2-4283.

5 REFERENCES

- B. Šuštaršič, I. Paulin, M. Godec, S. Glodež, M. Šori, J. Flašker, A. Korošec, S. Kores, G. Abramovič, Morphological and microstructural features of Al-based alloyed powders for powder-metallurgy applications, *Mater. Tehnol.*, 48 (2014) 3, 439–450
- ECKA Granules, <http://www.ecka-granules.com/en/ecka-granules/products/>
- Thermocalc software, <http://www.thermocalc.com/Software.htm>
- <http://www.netzsch-thermal-analysis.com/en/home.html>
- Netzsch: STA 449 F1: Simultaneous Thermal Analysis, Method, Technique, Applications, <http://private.netzschcdn.com/uploads/>
- International Standard ISO 2740-1986 (E), Sintered metal materials – Tensile test pieces, 1986-10-01, (connected with ISO 6892, Metallic materials- Tensile testing)
- J. F. Chinella, Z. Guo, Computational Thermodynamics Characterization of 7075, 7039, and 7020 Aluminum Alloys Using JMatPro, ARL, MD, USA, 2011
- Z. Guo, N. Saunders, A. P. Miodownik, J. P. Schillé, Prediction of room temperature mechanical properties in aluminium castings, Proceedings of the 7th Pacific Rim International Conference on Modeling of Casting and Solidification Processes, Dalian, China, 2007